VON KARMAN CENTER

STRUCTURAL MATERIALS DIVISION

STRESS-CORROSION CRACKING OF HIGH-STRENGTH ALLOYS

A REPORT TO

FRANKFORD ARSENAL

CONTRACT DA-04-495-ORD-3069

REPORT NO. 2914 (FINAL) / AUGUST 1964 / COPY NO. 5

AEROJET GENERAL TIRE GENERAL

CONTRACT FULFILLMENT STATEMENT

This final report is submitted in partial fulfillment of Contract DA-04-495-ORD-3069. It covers the period 1 July 1963 to 1 July 1964.

The investigation was performed at the Structural Materials Division Development Laboratories of Aerojet-General Corporation's Von Karman Center, Azusa, California.

The report was written by Mr. A. Rubin.

CONTENTS

CONTENTS (cont.)

V 1

CONTENTS (cont.)

I. OBJECTIVES

The objectives of this program are as follows:

A. To study the stress-corrosion characteristics of 18%-nickel maraging steel with respect to compositional variation.

B. To study the effect of environmental temperature on the rate of stress-corrosion cracking in three alloys: 18%-nickel maraging steel, a low-alloy martensitic steel, and a hot-worked die steel.

C. To study the electropotential changes occurring in 18%-nickel maraging steel during stress-corrosion exposure, and the effect of applied potential.

II. DISCUSSION

A. IMPORTANCE OF MARAGING STEELS

The maraging ultra-high-strength steels have attracted considerable attention in the aerospace industry since their introduction in 1961. The use of such steels appears particularly attractive for ultra-high-thrust rocket motor cases where large dimensions can greatly complicate metal fabrication and heat treatment. In such applications, maraging steels offer a number of advantages over conventional high-strength alloys. Most important, they do not require the quenching and tempering treatments that are characteristic of most ultra-high-strength alloys. Instead, they derive their high strength and characteristic toughness from a simple 850 to 900°F maraging heat treatment. In addition, maraging steels are weldable, with weldment properties approaching that of the parent material.

The maraging steel drawing foremost attention in the aerospace industry today is the alloy having a nominal composition of 18% nickel, 8%

cobalt, and 5% molybdenum. This alloy, referred to in this report as 18%-nickel maraging steel, is capable of attaining useful yield strengths in excess of 300,000 psi with exceptional ductility and toughness.

Before any alloy can be considered for rocket motor case applications, it must be demonstrated that the alloy has adequate resistance to stress-corrosion cracking under the conditions of its application. In fact, stress-corrosion cracking is the primary cause of premature failure of apparently metallurgically sound motor cases during hydrostatic testing and (to a lesser degree) in storage.

The present 1-year program, which constitutes the subject matter of this report, is part of a 2-year study of the stress-corrosion behavior of maraging steels. The first year's effort was largely concerned with determination of some basic environmental and material parameters which effect stress-corrosion cracking in 18%-nickel and 20%-nickel maraging steels. The second year's program involved the determination of the effects of compositional variation and environmental temperature on stress-corrosion cracking of 18%-nickel maraging steel as compared with a low-alloy martensitic steel and a hot-worked die steel.

B. STRESS-CORROSION CRACKING THEORY

Stress-corrosion cracking can be responsible for the sudden catastrophic failure of an alloy with otherwise excellent mechanical properties at stresses far below the material's yield strength. Such failures are induced by exposure of the alloy to specific environments while subjected to sustained stresses.

Although many theories of stress-corrosion cracking have been proposed, there are two principal mechanisms of interest: the continuous electrochemical process, and the alternate electrochemical-mechanical process. In the purely electrochemical process, crack propagation occurs by continuous anodic attack of the metal at the crack front; the second process proposes that a period of slow electrochemical attack alternates with fast mechanical fracture, leading to ultimate failure.

1. Electrochemical Mechanism

The electrochemical theory of stress corrosion was first proposed in 1940 by Dix (Reference 1). This theory states that the simultaneous action of the following three conditions will cause a metal to fail by stress corrosion:

a. A susceptibility to corrosion along continuous paths through the internal structure of the metal.

b. A corrosive environment making paths of susceptibility anodic to the matrix of the metal.

c. Applied or residual tensile stresses acting to pull the metal apart along these paths.

Cracking occurs in this case by selective electrochemical corrosion, with the tensile stresses acting to open fresh anodic sites. The above theory is directly applicable to intergranular cracking such as occurs in some aluminum alloys. The theory was subsequently extended to include transgranular cracking (Reference 2). In the case of transgranular cracking, the continuous paths are formed by slip planes and planes of precipitated constituents. Justification for this hypothesized mechanism is the measured increase in chemical activity along slip planes of plastically deformed crystals (Reference 3).

In other proposed electrochemical mechanisms it is stated that a prior existing path is not required. Uhlig (Reference 4) states that paths are continuously being formed due to plastic deformation at the tip of the advancing crack. He states that dislocation loops form zones in which interstitial elements such as nitrogen and carbon can deposit, forming cathodic sites. The mechanism may also account for the random branching paths observed in photomicrographs of stress-corrosion cracks.

A third electrical mechanism that is not as well accepted as those cited above involves strain-induced transformation at the tip of the advancing crack, the transformed structure being anodic to the remainder of the

metal. In mild steel, the transformed product is thought to be iron nitride (Reference 5); in austenitic stainless steel, the transformed product is thought to be martensite.

A fourth electrochemical mechanism is based on film rupture (References 6 and 7). The suggested sequence of events is as follows:

Electrochemical corrosion first causes grooves or notches to form on some portion of the stressed surface.

After some initiation period, the stresses at the tip of a notch become high enough to cause rupture of the naturally formed protective film.

Cracking proceeds because stress-induced film rupture causes anodic depolarization and dissolution of metal at the crack tip.

2. Mechanical Mechanisms

In each of the above mechanisms, the cracking proceeds by electrochemical dissolution of material. There have been other investigations which indicate that cracking was preceded, at least in part, by mechanical fracture.

Nielsen (Reference 8), in a study of oxides found in stress-corrosion cracks in stainless steel, states that formation of these oxides exerts sufficient lateral force to cause mechanical fracture at the root of the crack.

Edeleanu (Reference 9) and Keating (Reference 10) state that cracking proceeds by mechanical action with corrosion acting only to initiate the fracture. Microscopic studies by Edeleanu on migrating fractures indicate that crack propagation progresses by intermittent brittle fractures.

Although there is evidence both for and against the proposed mechanical and electrochemical modes of failure, there are two features of stress-corrosion cracking that are characteristic of any stress-corrosion process:

a. Cracks are formed under the combined action of stress and corrosion. They are not produced by the consecutive action of these agents.

b. The corrosive media which cause stress-corrosion cracking are very specific for a given alloy and are not necessarily related to purely chemical corrosivity of the alloy in the particular medium. In these two respects, stress-corrosion differs from fracture due to hydrogen embrittlement.

III. TEST METHODS

A. TEST SPECIMENS

1. Bent Beam Tests

The bent-beam test was the primary method used in this program. Figure 1 shows an insulated bent-beam fixture with test samples mounted. Polycarbonate blocks, 7.000 ±0.002 in. apart, attached to a stainless-steel holder support the test specimen and insulate it from the holder. Specimens were machined to exact lengths to produce a maximum calculated outer-fiber stress that amounts to 75% of the mean 0.2% offset yield strength. These length calculations are based on data supplied by the Research and Technology Division of the U.S. Steel Corporation. Figure 2 shows a representative plot of the stress-length relationships employed. These relationships were obtained by computer from U.S. Steel Co. formulas that resulted from a theoretically exact large-deflection analysis.

A four-point loading device was used to mount the specimens on the holder. The use of a four-point loading device in this pre-stressing operation eliminates possible local plastic deformation which can occur if the customary three-point loading method is used. Samples that were thus loaded into fixtures by the improved method and later released showed no measurable residual distortion, indicating that the yield strength of the material had not been exceeded during stressing.

Because of its simplicity, the bent-beam test lends itself well to the testing of a large number of specimens. A stress gradient is obtained along the specimen length with the maximum calculated stress approached at the longitudinal center.

2. U-Bend Tests

U-bend samples were used to show the effect of elastic stresses on stress-corrosion susceptibility. Figure 3 shows a typical U-bend sample bent around a 1-in. radius. Samples were bent after heat treatment by use of a special guide fixture.

3. Center-Notched Test

The specimen configuration used in the center-notch test is shown in Figure 4. It consists of a 1-3/4 by 8-in. tensile specimen containing a central notch, produced in a two-step process. In the first phase, a 0.06 by 0.57 in. slot is elox-machined and then extended at each end by very narrow elox-machined notches of 0.001-in. root radii. In the second phase, these notches are further extended by means of fatigue cycling to produce fatigue cracks of controlled dimensions.

The center-notched specimens are stress-corrosion tested in Baldwin creep-test machines (Figure 5). Dead-weight loading is applied to a 20:1 lever arm to give a K value at the crack tip of 75% of the K_c value. The test solution is applied in a plastic cup cemented to the specimen in the notched area before loading. An automatic timing device was used to record failure time.

When a specimen of this type is stressed, the elastic field parameter K (in ksi $\sqrt{\text{in.}}$) at the tip of the crack is represented by

$$K = \sigma \left(W \tan \frac{a}{W}\right)^{1/2}$$

where

W = specimen width (in.)

A = one-half of the total crack length (in.)

σ = nominal stress (ksi).

Simultaneously, the crack extension force (G_c) may be defined as follows:

$$G_c = \frac{K_c^2}{E}$$

where

E = material's elastic modulus

K_c = critical values of K at which crack propagation occurs in rapid tensile testing

From these relationships, the fracture toughness of the test materials was determined, using the center-notched specimens described above.

B. TEST ENVIRONMENTS

The test environments used were: (1) aerated distilled water, (2) aerated 3% NaCl solution, and (3) a high-humidity atmosphere, consisting of water-saturated air at 140°F. The pH of both the distilled water and the 3% salt solution was 7.0. Continuous aeration of baths was maintained with filtered air throughout the test duration in order to keep the environment constant with respect to oxygen. Control tests exposed to laboratory air were maintained at 70 to 78°F in a humidity range of 35 to 50%. No stress-corrosion failures have yet been encountered in the laboratory air, even with the most susceptible alloys.

Distilled water tests were conducted at both 120 $\pm$0.1°F and 160 $\pm$0.1°F, in addition to ambient temperature tests to determine the effect of temperature. All baths were changed every 10 days.

C. TEST MATERIALS

To study the effects of compositional variation on stress-corrosion susceptibility of 18%-nickel maraging steel, four different heats of material were evaluated. These heats, when taken in conjunction with the heats previously tested in the earlier part of the maraging-steel program, were selected to represent the compositional range of commercial production for this alloy. Materials were obtained from three suppliers: Republic Steel Corp., Vanadium Alloys Corp., and Latrobe Steel Corp.

Table 1 shows the composition of all materials studied. They include five heats of maraging steel from the previous year's program and four heats from the present program. The titanium content for these heats ranged from 0.23 to

1.40%, with yield strengths ranging from 181.5 to 232.3 psi. Heat treatments and mechanical properties are shown in Table 2. In addition to these materials, two alloys representing a hot-worked die steel and a low-alloy martensitic steel were tested to obtain comparison data. The various heat treatments and mechanical properties obtained for these alloys are also shown in Table 2.

D. SPECIMEN PREPARATION

The edges of all maraging-steel specimens were milled and the surfaces were vapor blasted using 400-mesh alumina powder after heat treatment. Chemical cleaning to remove heat treat scale was avoided to eliminate the possibility of chemical embrittlement. The alloy steel and the hot-worked die steel specimens were surface-ground 0.007-in. per side after final heat treatment to remove any decarburization that might be present.

For the evaluation of protective coatings, three coating systems were tested: a polyurethane system designated as X-500, an inorganic zinc system designated as No. 11, and an inhibited epoxy system designed as 454-1-1. These systems are commercially available. The coatings were applied by simple spray-on technique and cured at room temperature. Each coating was applied to beam-type specimens, cured, and the specimens then deflected to 75% of yield strength. Immersion tests were conducted in two media: a 3% NaCl solution, and 140°F water-saturated air. Uncoated control specimens were also immersed for comparison.

IV. TEST RESULTS

A. EFFECT OF COMPOSITION AND STRENGTH LEVEL

A total of nine heats of 18%-nickel maraging steel were tested. The only compositional constituent showing wide variation in these heats was titanium (see Table 1). This element was intended to be the compositional variable because its pronounced effect upon the mechanical properties of the alloy permits the attainment of a wide range of yield strengths (see Table 2). The titanium composition of the heats varied from 0.23% to 1.40%, with accompanying yield strengths varying from 181.5 to 323.3 ksi.

Results of the bent-beam and U-bend exposure tests are shown in Tables 3 and 4. It is noted, first, that all materials showed some failures, including the Republic Heat 3960523, which had the lowest titanium content (0.23%) and the lowest yield strength (181.5 ksi). In general, stress-corrosion susceptibility of 18%-nickel maraging steel increased with titanium content and strength level. For example, consider the bent-beam tests in the 140°F high-humidity air environment where there was stressing to 75% of yield strength. In these tests, the median failure time for the above-mentioned low yield-strength material (181.5 ksi yield) was 1560 hours, whereas the highest strength material tested (323.3 ksi yield) had a median failure time of 72 hours.

Figure 6 shows a graph of yield strength vs mean failure time for beam specimens in distilled water. The shorter failure times are obtained for the lower yield strength materials, and this applies to both maraging steel and to the conventional low-alloy steel and hot-worked die steel evaluated. Figure 6 also shows that at a given strength level, 18%-nickel maraging steel is less susceptible to failure than are the conventional high-strength steels.

Failure times shown in Table 4 for U-bend specimens indicate that the U-bend is a more severe test than the bent beam. Likewise, a comparison of distilled water exposures with 3% NaCl exposure generally indicates that distilled water is the more severe medium for inducing stress-corrosion failure in 18%-nickel maraging steel.

B. ENVIRONMENTAL TEMPERATURE

The effect of environmental temperature on stress-corrosion cracking of 18%-nickel maraging steel was determined using bent-beam and U-bend specimens in controlled distilled water environments at ambient temperature, at 120°F, and at 160°F. The temperature effect was shown to markedly increase the stress corrosion susceptibility of the alloy. The effect for U-bend specimens, as shown graphically in Figure 7, indicates a decrease in failure time of about 50% for an 18°F increase in temperature. The conventional high-strength steels tested for comparison, while showing a higher susceptibility to failure at room temperature, nevertheless showed little or no increase in susceptibility for

U-bend specimens as the temperature was raised from 70 to 160°F. This temperature effect was also borne out with bent-beam specimens of maraging steel, although failure times were considerably longer. The conventional steels again showed a higher susceptibility to failure than the maraging steel, and failure time decreased with temperature.

C. CENTER-NOTCHED SPECIMEN TESTS

It is generally believed that stress-corrosion cracking is a two-step process in which first a micro-notch must be formed by chemical means during an "incubative period" of stressed exposure to the environment. This step is then followed by a period of crack propagation which eventually results in fracture. The use of pre-notched test specimens for stress-corrosion testing supplies the initial notch (if it is sufficiently fine) from which crack propagation can take place. The resistance of an alloy to stress-corrosion cracking in the presence of a pre-notch is therefore of special interest. In service applications, some materials may have a pre-existing flaw or micro-crack which constitutes such a notch. The material's stress-corrosion resistance in such a case would be quite different from that which is determined by using unnotched test specimens.

Testing was performed in this program using the center-notched specimen configuration shown in Figure 3. The environment was applied to the specimen specifically in the notched area. Tables 6 and 7 show the results of these tests. In Table 6, the pH of a 3%-salt solution was varied from 3 to 11 in separate tests. The effect of making the solution more alkaline is shown to increase failure time for the maraging steels. The Republic alloy, RMS 200, shows the best resistance at all pH levels with no failures after 100-120 hours of exposure. Increased alkalinity of the solution had an especially marked effect in reducing susceptibility to stress-corrosion cracking for Vascomax 300 and 250 alloys. For example, with Vascomax 300, changing the pH of solution from 3 to 11 increased the failure time from 7.3 to 83.7 hours. The same pH change with Vascomax 250 altered the failure time from 29.6 hours to no failure after 140 hours. For Ladish D6ac alloy, the change in pH had little effect on failure times, which were generally shorter than for the maraging steels. Overall

failure times for all materials using center-notched specimens were shorter than for bent-beam specimens by at least a factor of 10. However, the general relationship still holds that stress-corrosion cracking susceptibility increases with yield strength.

Table 7 shows the effect of stress level on stress-corrosion cracking with the use of center-notched specimens. An increase in failure time is indicated as the stress level is decreased. For Ladish D6ac material, the varying susceptibility of the alloy for different tempering temperatures is shown. The exceptionally short stress-corrosion failure times for the B-1 material ($600^{\circ}F$ temper) emphasizes the importance of considering stress-corrosion susceptibility of an alloy with a given heat treatment when judging its useful strength.

D. ELECTROPOTENTIAL MEASUREMENTS

The electropotential study of stress-corrosion cracking of 18%-nickel maraging steel had two basic objectives: (1) to determine the effect of applied tensile stress on crack-tip corrosion potential, and (2) to determine the effect of applied potential on stress-corrosion cracking time.

A center-notched tensile specimen of the type shown in Figure 4 was used in the applied stress experiment with the setup as shown in Figure 8. The specimen, an 18%-nickel maraging steel sample with 250-ksi yield strength (Heat 396052), was exposed to a 3%-NaCl solution. A capillary tube, containing KCl solution in a gel, was used in this setup to contact the crack tip of the specimen, and lead to a calomel electrode. As the applied stress on the specimen was increased, voltage recordings were made to give the applied stress vs crack-tip corrosion potential relationships shown in Figure 9. This graph indicates that application of stress by incremental loading of the specimen causes a potential shift at the crack tip toward the cathodic side. If the stress-corrosion process is indeed electrochemical in nature, as has been frequently postulated, then the magnitude of such a shift would be expected to materially affect failure time. In fact, if the potential shift caused by the increased stress - rather than the stress itself - is the overriding factor in stress-corrosion cracking, then it should be possible by applying an external potential to the stressed specimen, to alter the failure time.

This theory was investigated in a second experiment to determine whether applied potential would affect failure time. Figure 10 shows the test setup for this portion of the program. A Duffers potentiostat is utilized to control the potential of a U-bend specimen to a predetermined value. The following data were developed when U-bend specimens of Heat 07868 were exposed to a 3%-NaCl solution:

Volts to Saturated Calomel Cell	Current Density ($ma/in.^2$)	Failure Time (hours)
-0.95	-3.6	2.1
-0.66	-2.0	168 NF
-0.36	-0.4	2.1
None (control)	None	2.3

It is seen that by applying the proper amount of cathodic current, stress-corrosion cracking of 18%-nickel maraging steel can be prevented. The current required to prevent failure is quite specific, and when it is increased over the critical value, the failure time is the same as with no current at all. These results afford strong evidence for an electrochemical mechanism of stress-corrosion cracking. It could be postulated that the specific current density which prevents stress-corrosion cracking is the one which makes the electrical potential of the "anodic path" (potential crack path in the material) and the surrounding metal matrix the same. There is, however, additional evidence that the electrochemical mechanism does not represent the complete picture. The failure of specimens in distilled water (which does not conduct a current to any appreciable extent) is difficult to explain on these grounds.

E. PROTECTIVE COATINGS

It was desired in the present program to evaluate the effectiveness and applicability of surface protection for preventing stress-corrosion cracking of 18%-nickel maraging steel. Three coating systems which had been effective in preventing stress-corrosion cracking of H-11 steel in the first year's program were evaluated for use with maraging steel

Each of the three coating systems offers a different means of protecting the base metal. The polyurethane coating forms a dense barrier between the environment and the metal. The inorganic zinc coating serves to provide cathodic protection for the base metal, and the inhibited epoxy coating protects the metal by inhibitory action of chromate compounds as well as by forming a barrier against the environment.

Table 5 shows the results of these tests. When applied to H-11 steel (heat-treated to a stress-corrosion susceptible condition), the inhibited epoxy coating (No. 454-1-1) showed excellent protective ability in preventing failure in a 3%-salt solution after 3100 hours of exposure. With the polyurethane system X-500, the steel failed in 1380 hours. With the Zinc-11 coating, failure occurred in 687 hours. The base metal failed under the same conditions in 1.5 hours, when no coating was applied.

When applied to 18%-nickel maraging steel, the inhibited epoxy coating again showed no failures - in this case after 4990 hours of exposure. The polyurethane system was also very effective with 4488 hours of exposure before failure occurred in one specimen. Two other specimens did not fail in 4990 hours. The inorganic zinc coating prevented base-metal failure for only 288 hours. The uncoated base metal (18%-nickel maraging steel) had a median failure time of 119 hours.

The same coating systems were also tested in 140°F water-saturated air. The inhibited epoxy coating again showed excellent protective ability on both H-11 steel and on maraging steel, although results were not quite as impressive as for the salt-solution exposure. The polyurethane coating again appeared promising, while the zinc coating was very poor, especially on maraging steel where acceleration of bare-metal failure time was actually obtained.

Figures 11 to 23 represent a series of macrographs, micrographs, and electron microscope fractographs of typical grain structures and crack patterns associated with stress-corrosion failures in 18%-nickel maraging steel and H-11 steel samples. The descriptions of the views taken are shown below the photographs. The mode of cracking was intergranular.

V. SUMMARY AND CONCLUSIONS

Based on results obtained in the second year's program to investigate the stress-corrosion susceptibility of 18%-nickel maraging steel, the following conclusions can be drawn:

A. Susceptibility to stress-corrosion failure ~~is~~ was found in all 18%-nickel alloy heats having yield strengths from 181.5 to 232.2 ksi. Susceptibility ~~becomes~~ became greater with increasing titanium content and yield strength.

B. At a given strength level, 18%-nickel maraging steel ~~is~~ was less susceptible to failure than ~~is~~ was H-11 steel or a hot-worked die steel. Cold working of 18%-nickel maraging steel before aging further reduces its susceptibility to stress-corrosion failure.

C. Distilled water ~~is~~ was a more severe exposure medium than 3%-salt water in causing corrosion cracking, and the U-bend test ~~is~~ was more severe than the bent-beam test - at least with regard to 18%-nickel maraging steel.

D. The 18%-nickel maraging steel showed a marked increase in susceptibility to stress-corrosion cracking with an increase in environmental temperature. ~~By comparison, conventional high-strength steels at the same stress level h~~ had ~~a higher susceptibility to failure at room temperature, but show a lesser increase in susceptibility with temperature rise.~~

E. An inhibited epoxy coating designated as 454-1-1 was very effective in greatly delaying stress-corrosion cracking both of maraging steels and of H-11 steel. An inorganic zinc coating designed to impart cathodic protection was found to be ineffective.

F. An electrochemical mechanism for failure of maraging steel in 3%-NaCl solution ~~has been~~ was demonstrated by the preventing of stress-corrosion failure upon application of cathodic current.

G. ~~Stress-corrosion susceptibility of maraging steel increases with acidity and decreases~~ with alkalinity of the exposure solution.

REFERENCES

1. E. H. Dix, Jr., "Acceleration of the Rate of Corrosion by High Constant Stresses," Trans. AIME, 137, 11 (1940).

2. R. B. Mears, R. J. Brown, and E. H. Dix, "A Generalized Theory of Stress Corrosion of Alloys," Symposium on Stress Corrosion of Alloys, ASTM, AIME, 323 (1945).

3. H. W. Paxton, R. E. Reed and R. Leggett, "Stress Corrosion of Single Crystals of Stainless Steel," Physical Metallurgy of Stress Corrosion Cracking, Interscience, 181 (1959).

4. H. H. Uhlig, "New Perspectives in the Stress Corrosion Problem," Physical Metallurgy of Stress Corrosion Fracture, Interscience, 1 (1959).

5. J. T. Waber and H. J. McDonald, Stress Corrosion Cracking of Mild Steel, Corrosion Publishing Co. (1947).

6. J. G. Hines, "On the Propagation of Stress Corrosion Cracks in Metal," Corrosion Science, I, 21 (1961).

7. H. L. Logan, "Film Rupture Mechanism of Stress Corrosion," J. Res. N.B.S., 48, 99 (1952).

8. H. A. Nielsen, "The Role of Corrosion Products in Crack Propagation in Austenitic Stainless Steels. Electron Microscopic Studies," Physical Metallurgy of Stress Corrosion Fracture, Interscience, 121 (1959).

9. C. Edeleanu, "Crack Propagation Along Stress Corrosion," Physical Metallurgy of Stress Corrosion Fracture, Interscience, 79 (1959).

10. F. H. Keating, "Internal Stresses in Metals and Alloys," Inst. Met. Lord., 311 (1948).

TABLE 1

MILL-CERTIFIED CHEMICAL ANALYSIS OF PROGRAM MATERIALS

Supplier	Heat No.	Composition, %														
		C	Mn	P	S	Si	Ni	Co	Mo	Al	Cr	Zr	Ti	Ca	B	V
*(a) Maraging Steel from First Year Program																
Republic Steel	3960502	0 02	0.08	0.007	0.006	0.15	18.48	7.00	4.84	0.21	0.10	0.035	0.50	-	0.0036	-
Allegheny-Ludlum	448	0.029	0.002	0.004	0.008	0.009	18.51	8.48	4.92	0.089	-	-	0.52	-	-	-
Allegheny-Ludlum	W-24178	0.012	0.01	0.003	0.005	0.01	18.69	8.90	4.92	0.029	-	0.003	0.62	0.006	0.002	-
Allegheny-Ludlum	476	0.02	0.08	0.006	0.005	0.014	18.60.	9.05	4.90	0.078	-	-	1.00	-	-	-
Allegheny-Ludlum	W.24254	0.009	0.09	0.002	0.005	0.06	20.41	-	-	0.29	-	0.002	1.40	0.004	0.003	-
(b) Maraging Steel for Present Program																
Republic Steel	3960523	0.029	0.06	0.005	0.006	0.05	17.79	8.50	3.48	0.13	-	-	0.23	-	-	-
Vanadium Alloys	07868	0.02	0.09	0.004	0.005	0.10	17.75	7.60	4.60	0.08	-	0.017	0.52	0.05	0.004	-
Latrobe Steel	C56858	0.03	0.03	0.004	0.008	0.05	18.34	8.00	4.75	0.11	-	0.03	0.49	-	0.004	-
Vanadium Alloys	07268	0.03	0.05	0.004	0.006	0.04	18.54	9.06	4.88	0.09	-	0.088	0.55	0.02	0.003	-
(c) Conventional High-Strength Steels																
Vanadium Alloys	07914	0.38	0.21	0.010	0.008	0.92	-	-	1.33	-	4.75	-	-	-	-	0.51
Allegheny-Ludlum	W-23217	0.495	0.62	0.009	0.003	0.20	0.57	-	0.94	-	1.00	-	-	-	-	0.05

*Some material from previous year's program was used to obtain supplementary data.

TABLE 2

MECHANICAL PROPERTIES OF PROGRAM MATERIALS

Code No.	Heat No.	Prior Condition	Heat Treatment Temp, °F	Heat Treatment Hold, hours	0.2% Offset Yield Strength ksi	Ultimate Tensile Strength	Elongation %	Reduction in Area %	R_c Hardness	ASTM Grain Size No.	Crack Growth Energy (G_c) lb/in.^{2}
H-1	W-24254	Annealed	850	4	291.3	302.2	3	17	54	15	59
H-2	↓	50% CR*	↓	↓	321.0	327.1	3	25	55-1/2	-	22.9
H-3	↓	75% CR	↓	↓	298.3	308.8	2-1/2	13	55	-	15.8
H-W	W-24254	Welded	850	4	245.0	252.0	1-1/2	5	-	-	-
I-5	477	50% CR	900	3	278.0	280.7	2	8	51-1/2	-	483
I-4	3960502	Annealed	↓	↓	249.9	254.7	4	37	50-1/2	12	825
I-2	↓	50% CR	↓	↓	302.5	308.1	4	26	52-1/2	-	343
I-W	3960502	Welded	↓	↓	236.6	242.0	2	20	-	-	-
I-6	448	Annealed	↓	↓	255.4	265.9	5	9	52	13-1/2	760
I-7	448	50% CR	↓	↓	331.0	332.5	1-1/2	7	55	-	(573)
I-3	W-24178	Annealed**	↓	↓	283.0	294.0	8	38	53-1/2	-	625
I-1	W-24178	50% CR	↓	↓	323.8	328.4	1-1/2	28	55	-	228
I-8	476	Annealed	↓	↓	323.3	330.0	2-1/2	27	56	14-1/2	430
I-9	476	50% CR	900	3	354.4	354.9	1	1-1/2	58	-	159
K	3960523	Annealed	900	3	181.5	190.7	5	43	42	8	1020
L	07868	↓	↓	↓	248.2	(248.2)	4	-	49	12-1/2	857
M	C56858	↓	↓	↓	269.7	275.7	5	34	51-1/2	7-1/2	755
N	07268	Annealed	900	3	279.1	288.1	4	18	52	12-1/2	639
A-4	07914	1 hr, 1850°F, OQ**	1075	4 + 4	219.2	257.7	7	44	49	-	-
A-3	↓	↓	1025	↓	232.6	284.8	6	42	52-1/2	-	-
A-2	↓	↓	975	↓	223.5	280.6	6-1/2	43	53	-	46.0
A-1	07914	1 hr, 1850°F, OQ	925	4 + 4	222.2	292.4	7	40	54	-	33.5
B-4	W-23217	40 min, 1550°F, OQ	1100	2	203.1	218.5	11	46	44	-	785
B-3	↓	↓	900	↓	204.6	226.4	7-1/2	43-1/2	44	-	446
B-2	↓	↓	800	↓	214.5	241.2	7	38	45-1/2	-	374
B-1	W-23217	40 min, 1550°F, OQ	600	2	237.4	281.3	6	25	51-1/2	-	192

NOTES: *CR - Cold reduced at mill

**Received cold reduced, annealed 1 hour at 1500°F, air cooled.

***OQ = Oil Quenched.

Report No. 2914

Table 2

TABLE 3

BENT-BEAM STRESS-CORROSION TEST RESULTS

Material (Table 2 Code No.)	Heat Number	0.2% Offset Yield Strength (ksi)	Failure Ratio* and Failure Time (Hours)** In Various Environments: Distilled Water Ratio	Distilled Water Time	3%-NaCl Solution Ratio	3%-NaCl Solution Time	120°F Distilled Water Ratio	120°F Distilled Water Time	140°F Water-Saturated Air Ratio	140°F Water-Saturated Air Time	160°F Distilled Water Ratio	160°F Distilled Water Time
(a) Maraging Steel from Previous Program, Mill-Annealed												
H-1	W-24254	291.3	3/3	10.5	3/3	7.8	0/0	-	3/3	105	2/2	47
I-4	3960502	249.9	3/3	70	3/3	140	3/3	164	3/3	475	3/3	138
I-6	448	255.4	1/3	NF 3600	0/2	NF 3600	0/0	-	3/3	266	1/1	355
I-1	W-24178	283.0	3/3	36	3/3	36	2/2	145	3/3	21.5	2/2	16
I-8	476	323.3	3/3	24	2/2	6.5	1/1	120	3/3	72	0/0	-
(b) Maraging Steel from Previous Program, Welded												
H-W	W-24254	245.0	3/3	47	3/3	0.8	2/2	42	3/3	14	2/2	15
I-W	3960502	236.6	3/3	360	3/3	115	2/2	148	3/3	139	2/2	31
(c) Maraging Steel, 50% Cold Reduced												
H-2	W-24254	321.0	1/3	NF 2900	0/3	NF 2900	2/2	810	3/3	5800	2/2	138
I-5	477	278.0	0/3	NF 3600	0/2	NF 3600	0/0	-	2/3	5800	1/1	1010
I-2	3960502	302.5	3/3	1780	2/3	3200	2/2	256	3/3	380	2/2	150
I-7	448	331.0	0/3	NF 3600	0/2	NF 3600	0/1	NF 1000	3/3	3080	1/1	690
I-3	W-24178	323.0	4/4	536	3/3	1580	2/2	473	3/3	290	2/2	186
I-9	476	354.4	3/3	4460	2/2	20	1/1	304	3/3	930	1/1	136
(d) Maraging Steel from Present Program												
K	3960523	181.5	0/3	NF 5080	0/3	NF 5712	3/3	3095	3/3	1560	3/3	740
L	07868	248.2	3/3	1032	0/3	NF 5040	3/3	596	3/3	578	3/3	300
M	C-56858	269.7	3/3	3190	3/3	1940	3/3	324	3/3	188	3/3	138
N	07268	279.1	3/3	510	3/3	119	3/3	336	3/3	535	3/3	138
(e) Conventional High-Strength Steels												
A-4	07914	219.2	1/2	1828	2/2	853	2/2	784	1/2	2852	2/2	584
A-3	07914	232.6	2/2	544	2/2	416	2/2	198	2/2	1652	2/2	196
A-2	07914	223.6	2/2	294	2/2	179	2/2	138	2/2	166	2/2	160
A-1	07914	222.2	3/3	143	3/3	18	4/4	82	3/3	482	2/2	73
B-4	W-23217	203.1	0/3	NF 3984	0/2	NF 4700	0/2	NF 3976	0/2	NF 3976	0/2	3144
B-3	W-23217	204.6	3/3	2432	0/3	NF 4700	3/3	2825	3/3	908	2/2	500
B-2	W-23217	214.5	3/3	1200	3/3	3230	3/3	700	3/3	309	2/2	198
B-1	W-23217	237.4	3/3	720	1/3	NF 4464	3/3	213	3/3	141	2/2	103

NOTE: All specimens stressed to 75% of yield strength. *Ratio of samples failed to samples tested.
**Median failure times in hours for three specimens or average for two specimens.

TABLE 4

U-BEND STRESS-CORROSION TEST RESULTS

Material (Table 2 Code No.)	Heat No.	0.2% Offset Yield Strength	Failure Ratio* and Failure Time, Hours,** in Various Environments									
			Aerated Distilled Water		Aerated 3% NaCl Solution		120°F Distilled Water		140°F Water-Saturated Air		160°F Distilled Water	
			Ratio	Time	Ratio	Time	Ratio	Time	Ratio	Time	Ratio	Time
			(a) Maraging Steel from Previous Program									
H-1	W-24254	291.3	2/2	3.4	2/2	2.4	3/3	194	0/0	--	3/3	46
I-4	3960502	249.9	2/2	825	0/0	--	2/2	133	2/2	167	3/3	20
			(b) Maraging Steel from Present Program									
K	3960523	181.5	3/3	2140	1/3	NF 4150	3/3	333	4/4	240	3/3	130
L	07868	248.2	3/3	620	3/3	1776	3/3	191	3/3	167	3/3	40
M	3960858	269.7	3/3	430	3/3	1174	3/3	237	3/3	70	3/3	20
N	07268	279.1	2/3	1823	3/3	4704	3/3	410	3/3	470	2/2	35
			(c) Conventional High Strength Steels									
A-4	07914	219.2	2/2	510	2/2	267	2/2	280	2/2	500	2/2	330
A-3	↓	232.6	2/2	174	2/2	232	2/2	172	2/2	30	1/1	232
A-2	↓	223.5	2/2	200	2/2	143	2/2	119	2/2	70	2/2	144
A-1	07914	222.2	2/2	82	2/2	24	2/2	70	2/2	24	2/2	51
B-4	W-23217	203.1	1/2	NF 4176	0/2	NF 4176	0/2	NF 4176	0/2	NF 4176	0/1	NF 3120
B-3	↓	204.6	2/2	1470	0/2	3348	2/2	974	2/2	372	1/1	620
B-2	↓	214.5	2/2	144	2/2	2600	2/2	537	2/2	217	1/1	380
B-1	W-23217	237.4	2/2	4.9	2/2	1.0	2/2	2.4	2/2	<1	1/1	<1

Notes: All specimens stressed beyond yield strength.

* Ratio of samples failed to samples tested.

** Median failure times for three specimens, average for two specimens.

TABLE 5

BENT-REAM STRESS-CORROSION TESTS FOR COATINGS EVALUATION

Base Metal	Coating	3%-NaCl Solution		140°F Water-Sat. Air	
		Failure Ratio*	Median Failure Time (Hours)	Failure Ratio*	Median Failure Time (Hours)
H-11 Steel	None	4/4	1.5	2/2	64
H-11 Steel	Polyurethane X-500	3/3	1380	6/6	3500
H-11 Steel	Inorganic Zinc - 11	2/2	687	2/2	821
H-11 Steel	Inhibited Epoxy 454-1-1	0/2	NF 3100	3/3	2720
18%-Nickel Maraging Steel	None	3/3	119	3/3	535
18%-Nickel Maraging Steel	Polyurethane X-500	1/3	488	3/3	1560
18%-Nickel Maraging Steel	Inorganic Zinc - 11	3/3	288	3/3	140
18%-Nickel Maraging Steel	Inhibited Epoxy 454-1-1	0/3	NF 4990	2/3	1870

*Ratio of samples failed to samples exposed.

TABLE 6

EFFECT OF pH VARIATION ON STRESS-CORROSION CRACKING
(Center-Notched Specimens Exposed to 3%-Salt Solution)*

Material	Table 2 Code	Notched Tensile Strength (psi)	pH	Failure Time (Hours)
Vascomax 300	N	180,000	3	7.3
	N	180,000	5	43.4
	N	180,000	9	32.9
	N	180,000	11	83.7
Republic RMS 200	K	191,000	3	100 (NF)**
	K	191,000	5	110 (NF)
	K	191,000	9	118 (NF)
	K	191,000	11	120 (NF)
Vascomax 250	L	205,300	3	29.6
	L	205,300	5	31.8
	L	205,300	9	90.1
	L	205,300	11	140 (NF)
Marvac 18	M	196,400	3	26.7
	M	196,400	5	35.8
	M	196,400	9	46.9
	M	196,400	11	53.9
Ladish D6ac	B-4	196,800	3	42.0
	B-4	196,800	5	60.9
	B-4	196,800	9	44.3
	B-4	196,800	11	44.6

*Stress = 75% of Notched Tensile Strength

**NF = No Failure.

TABLE 7

EFFECT OF STRESS LEVEL ON STRESS-CORROSION CRACKING

(Center-Notched Specimens Exposed to 3% Salt Solution)

Material	Table 2 Code	Stress Level - Percent of Notched Tensile Strength	Failure Time* (Hours)
Republic RMS 200	K	75	50.0 (NF)**
		65	94.5 (NF)
		65	13.9 (NF)
Marvac 18	M	75	12.2
		75	20.0
		65	58.7
		55	50.5
		50	53.7 (NF)
Vascomax 250	L	75	29.0
		75	29.9
		65	65.9
		65	20.6
		55	80.5
		50	81.5
Vascomax 300	N	75	20.2
		75	33.4
		55	46.9
		50	45.4
		50	53.7 (NF)
Ladish D6ac	B-4	85	22.0
		70	73.8
		70	50.7 (NF)
	B-3	75	1.4
		75	1.1
		37	4.1
		30	3.5
		25	8.3
		25	9.1
		20	9.4
	B-2	75	61.8 min
		75	32.5 min
		75	34.6 min
		75	28.2 min
		37	2.8 hours
		18	2.3 hours
		12	53.5 hours (NF)
		12	71.1 hours (NF)
	B-1	75	4.2 min
		37	2.6 hours
		18	72.0 hours

*Failure time in hours, except where otherwise specified.

**NF = No Failure

22

2

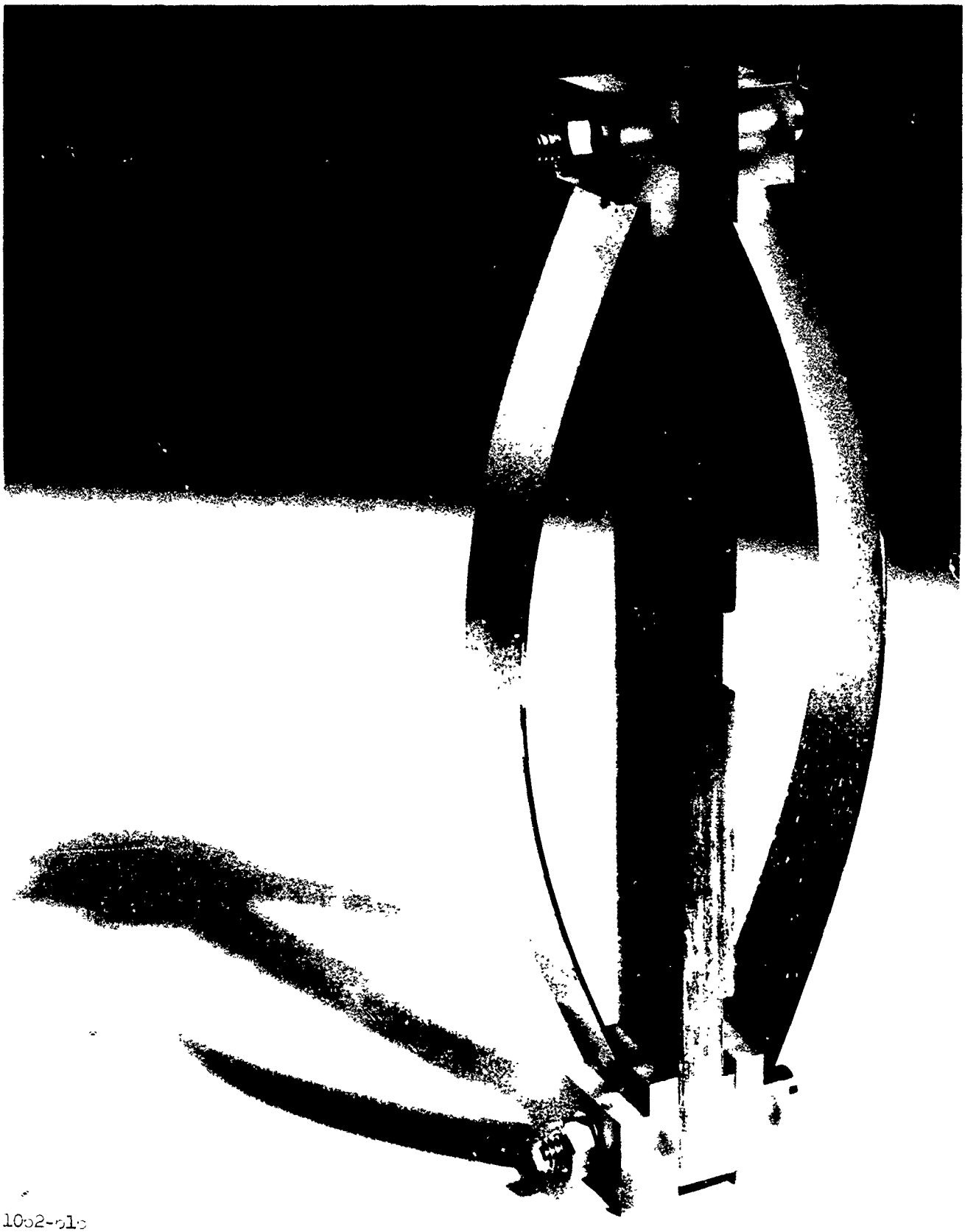

1052-61c

Bent-Beam Test Fixture and Specimens

Figure 1

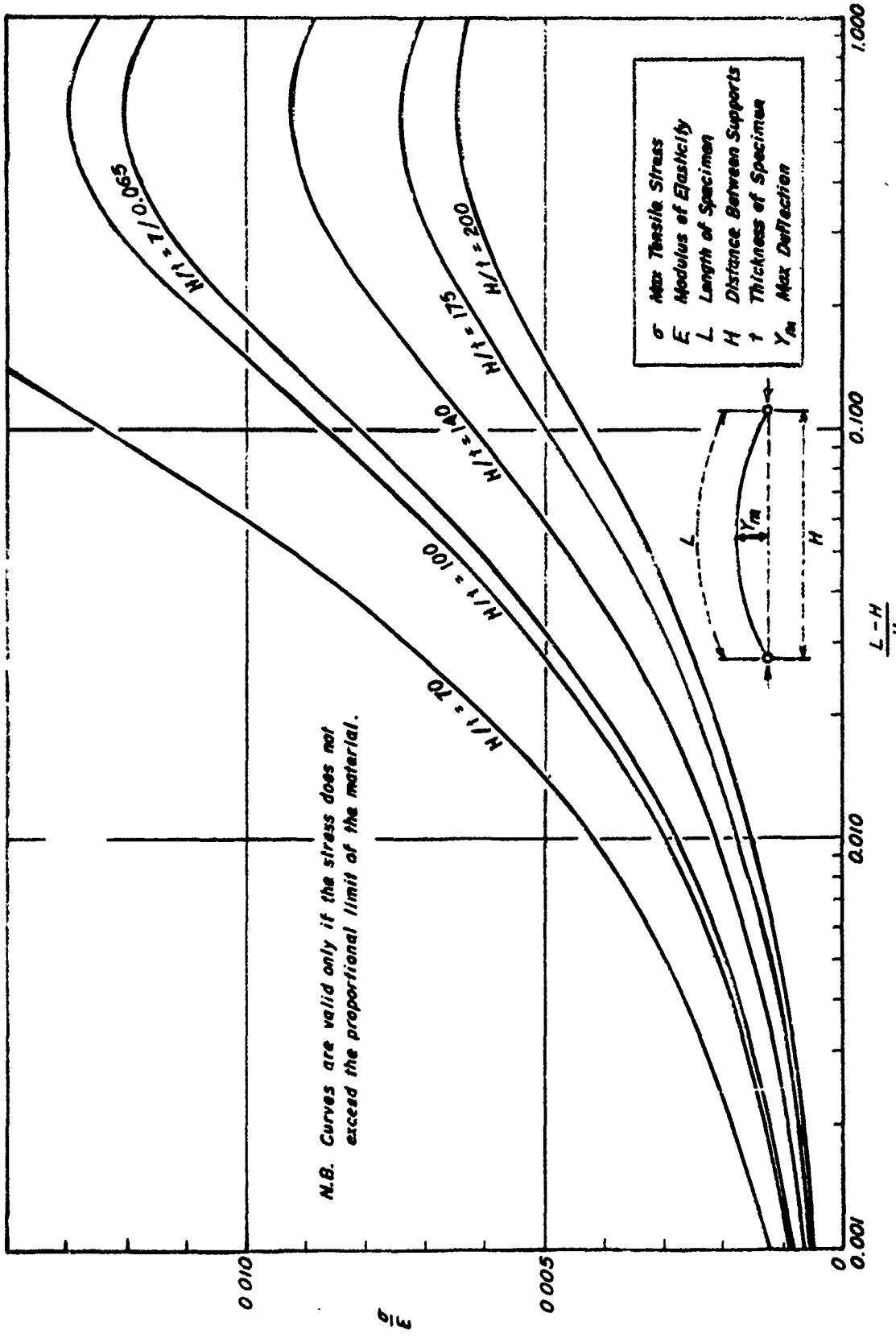

Beam Length-Stress Relationship

Figure 2

U-Bend Test Specimen

Figure 3

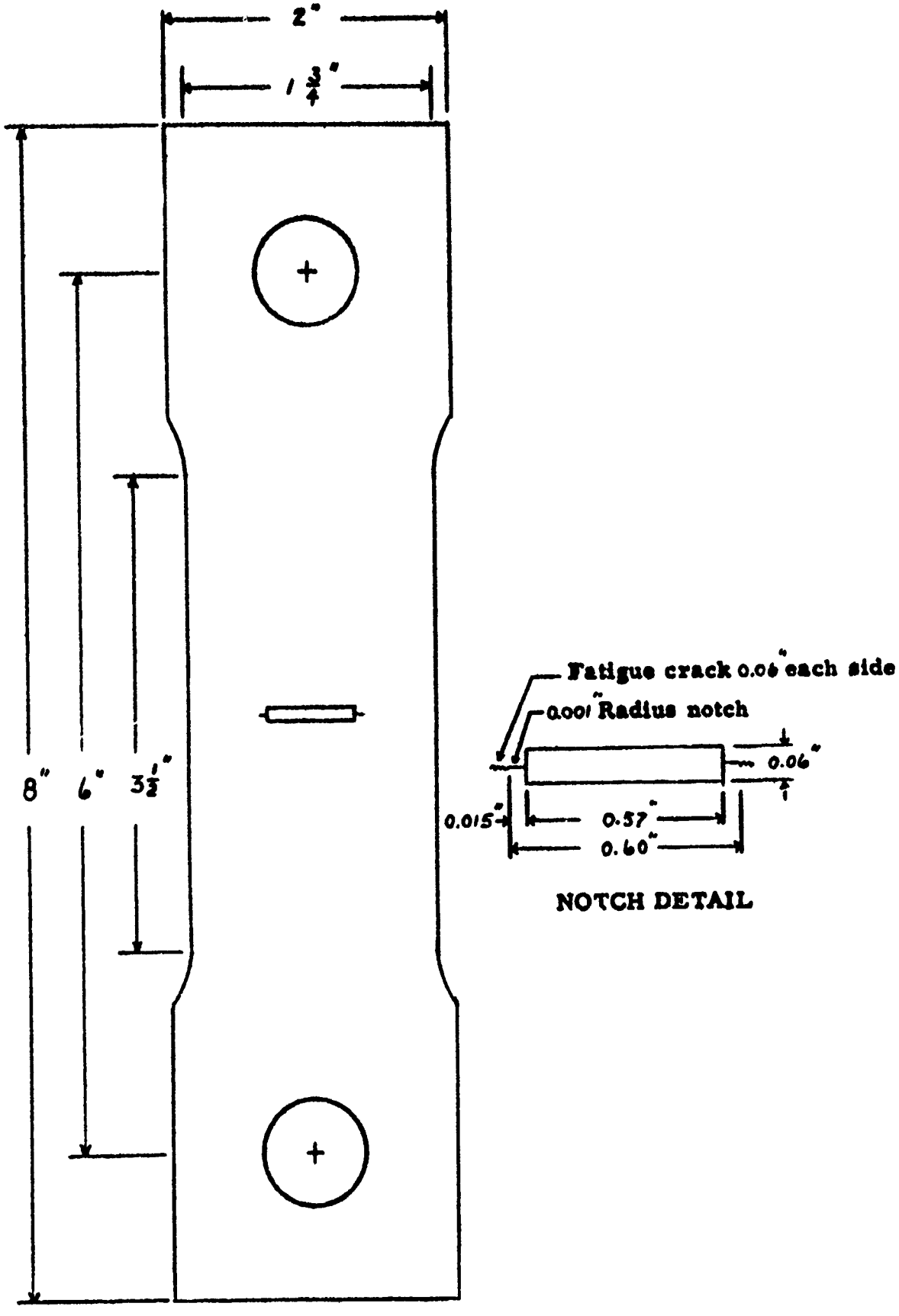

Center-Notched Specimen Configuration

Figure 4

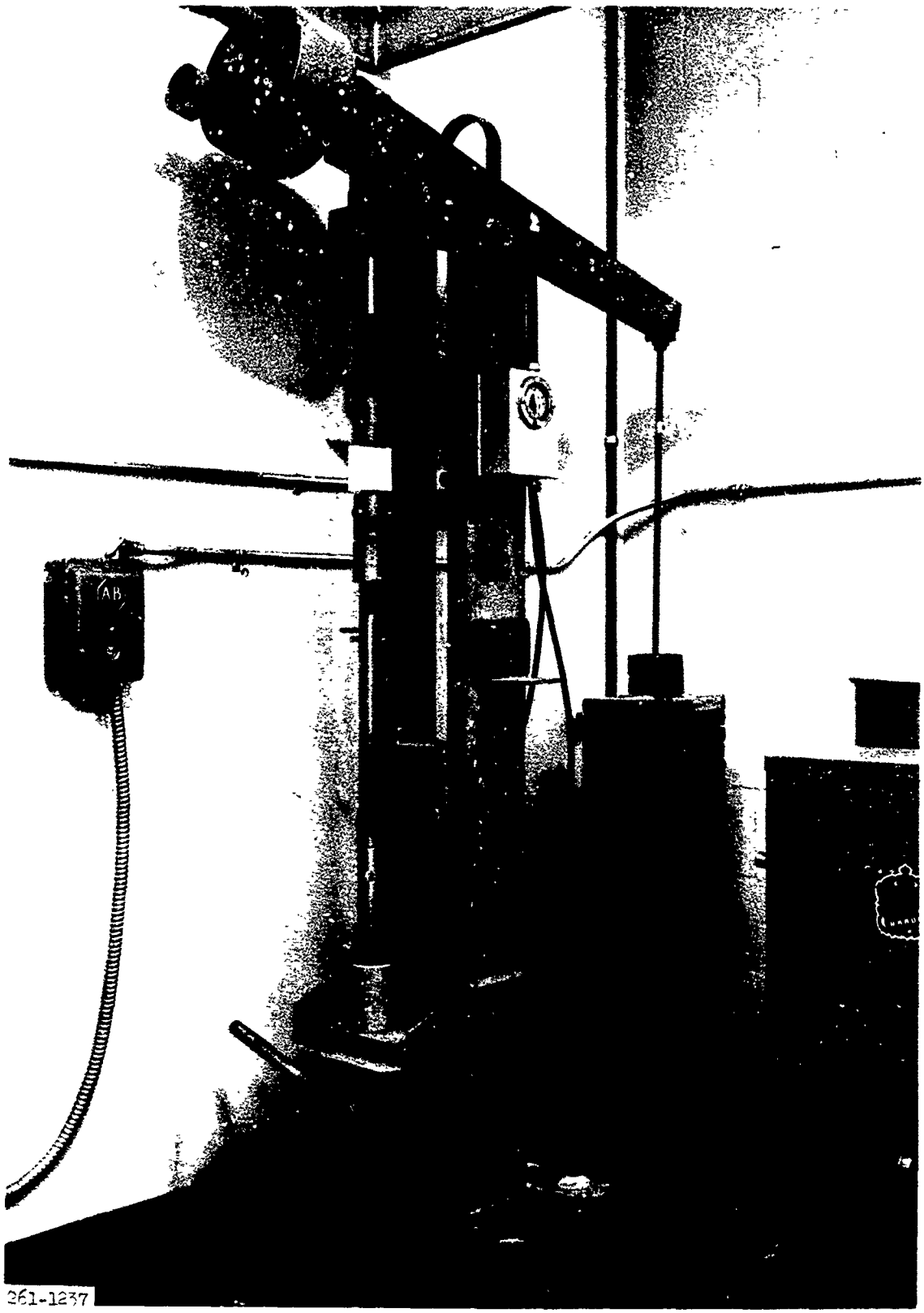

Stress-Corrosion Test Setup for Center-Notched Specimens

Figure 5

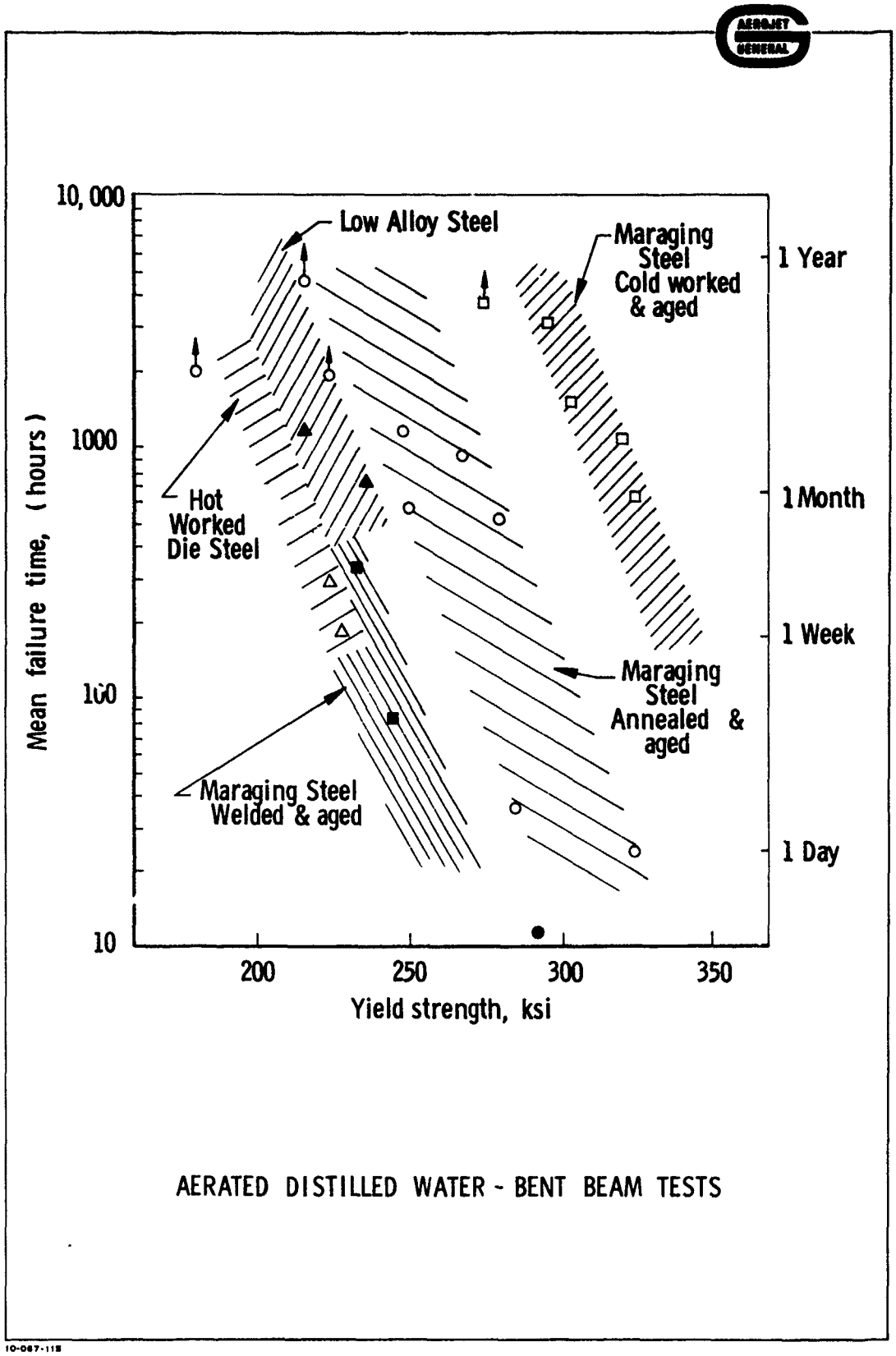
10,000
1000
100
10
Mean failure time, (hours)
Low Alloy Steel
Maraging Steel Cold worked & aged
Hot Worked Die Steel
Maraging Steel Annealed & aged
Maraging Steel Welded & aged
1 Year
1 Month
1 Week
1 Day
200
250
300
350
Yield strength, ksi
AERATED DISTILLED WATER - BENT BEAM TESTS
10-067-11B

Figure 6

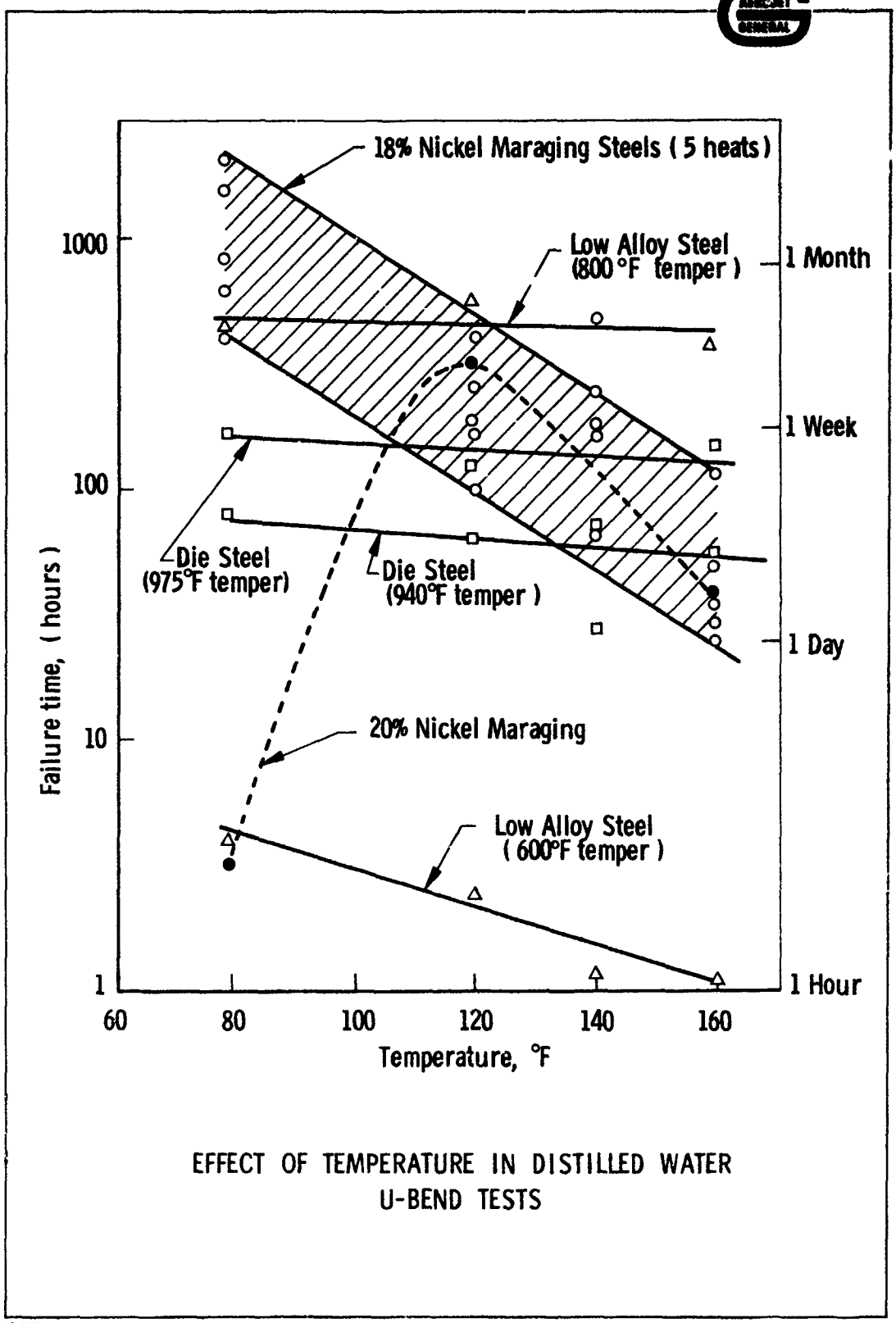

EFFECT OF TEMPERATURE IN DISTILLED WATER
U-BEND TESTS

10-067-118

Figure 7

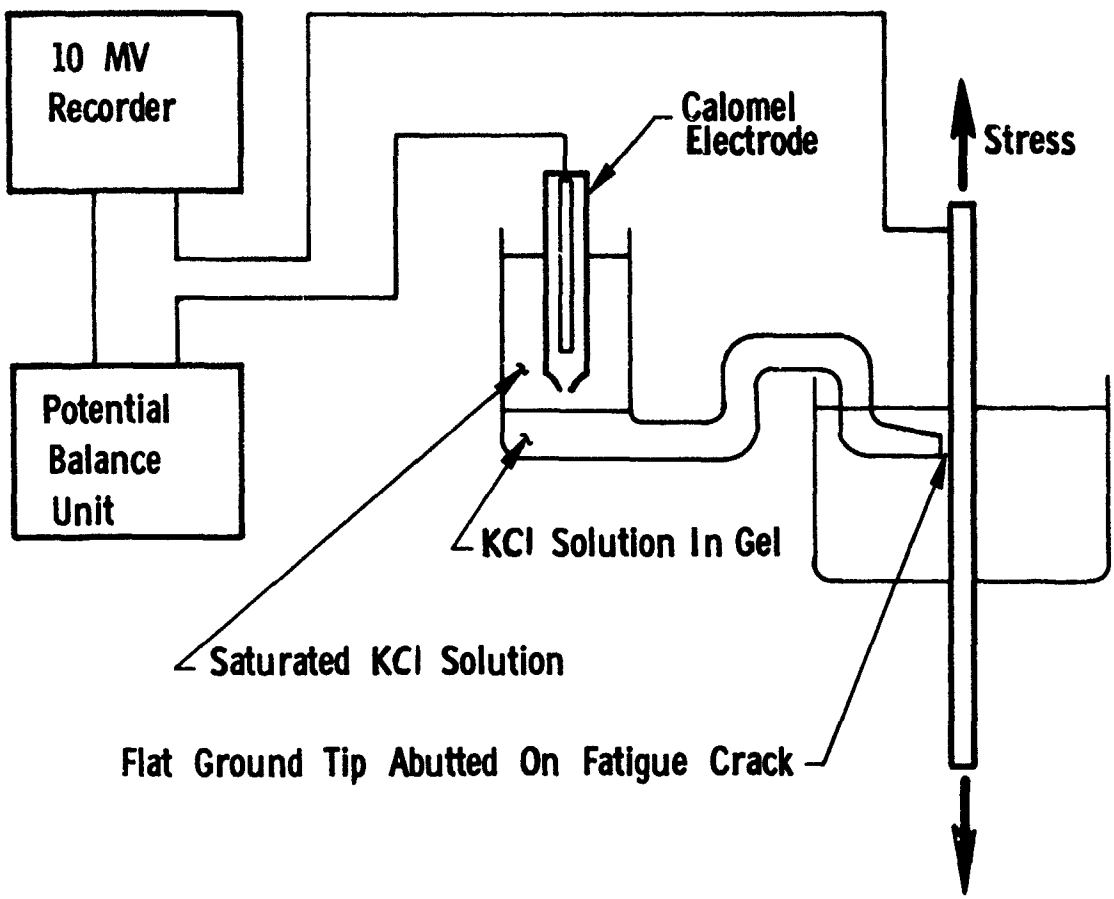

STRESS-CORROSION POTENTIAL MEASURING APPARATUS

Figure 8

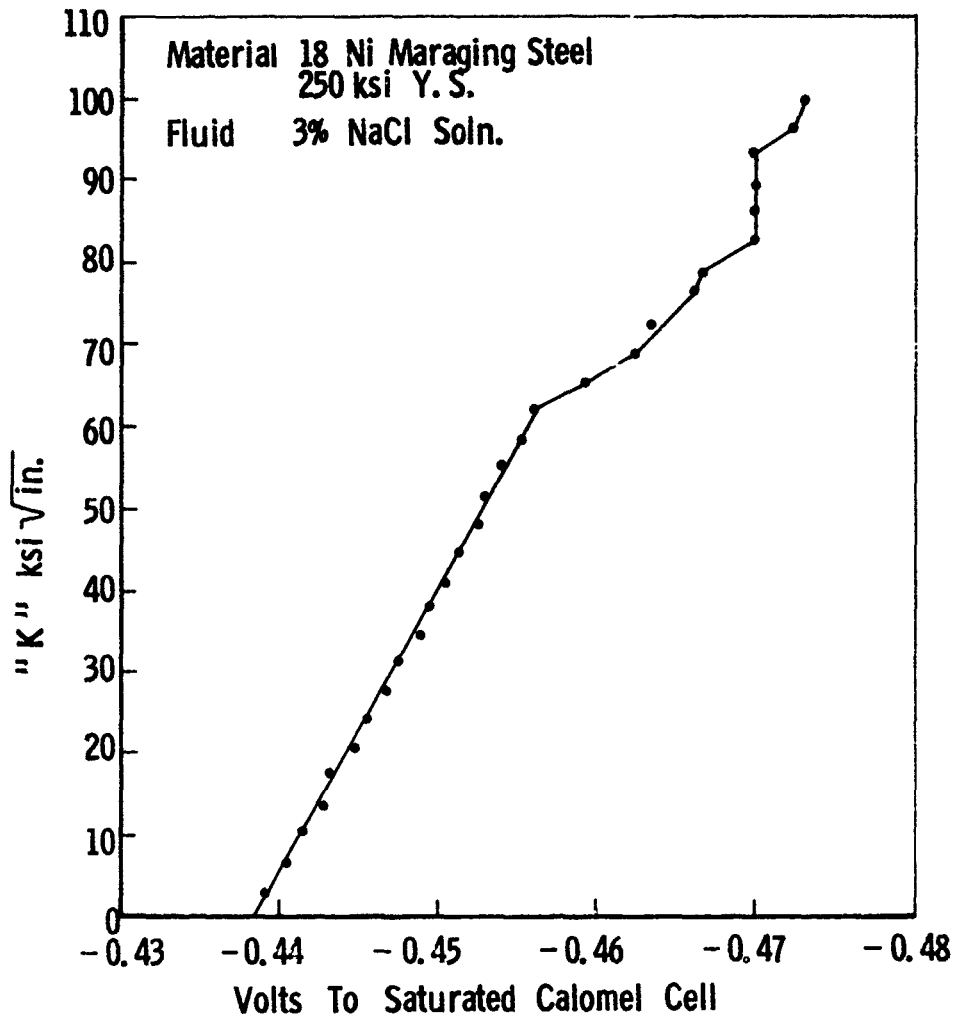

EFFECT OF STRESS FIELD PARAMETER, K, ON CRACK-TIP CORROSION POTENTIAL

Figure 9

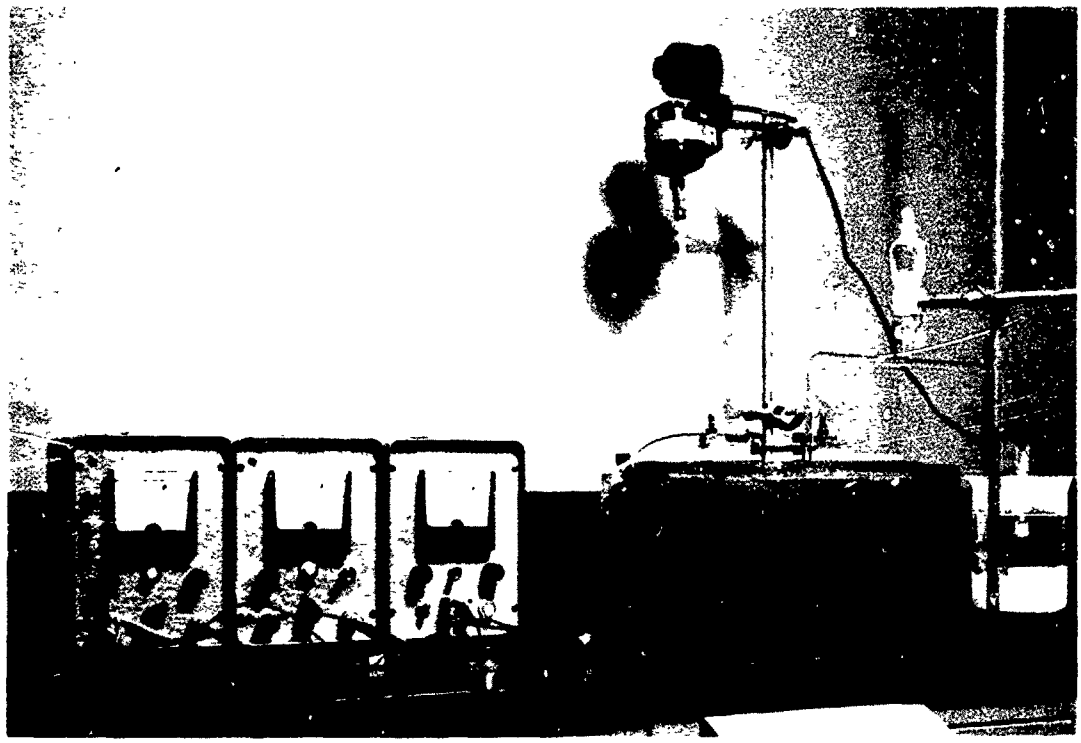

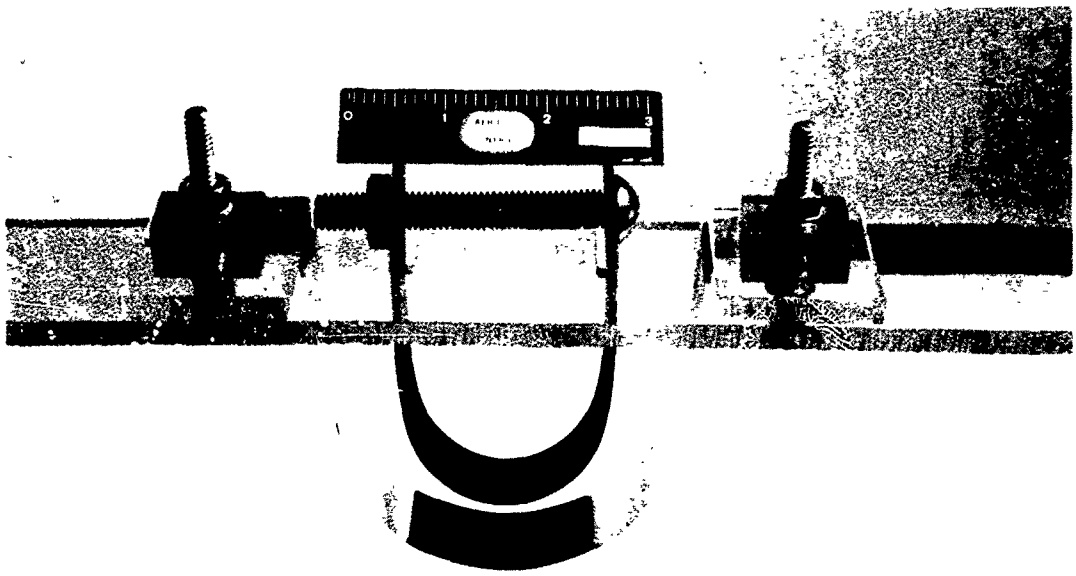

(Top) Experimental Test for the Determination of Applied Potential Effect on Stress-Corrosion Cracking

(Bottom) Test Cell Showing Specimen and Auxiliary Platinum Electrode

Figure 10

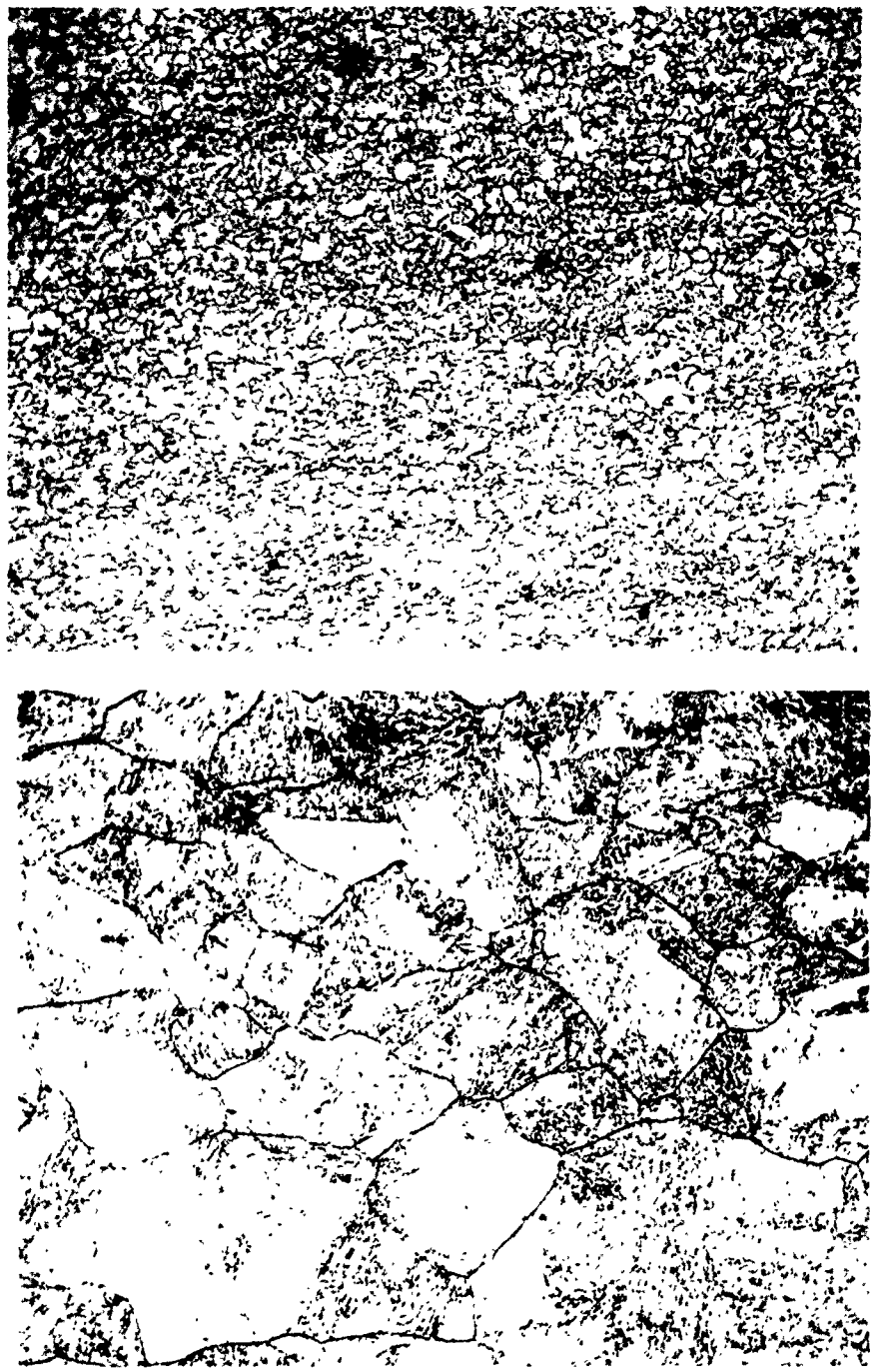

Grain Size Variations Encountered in 18% Nickel Maraging Steels

(Top) Heat 476 (Bottom) Heat 3960523

Etchant: 5% chromic acid, electrolytic

Magnification: 500X

Figure 11

Typical Stress-Corrosion Crack in 18% Nickel Maraging

Heat 3960523

Etchant: Dilute marbles

Magnification: 1400X

Figure 12

Surface of Annealed-and-Aged 18% Nickel Maraging Steel Crack (Approx. 1X)

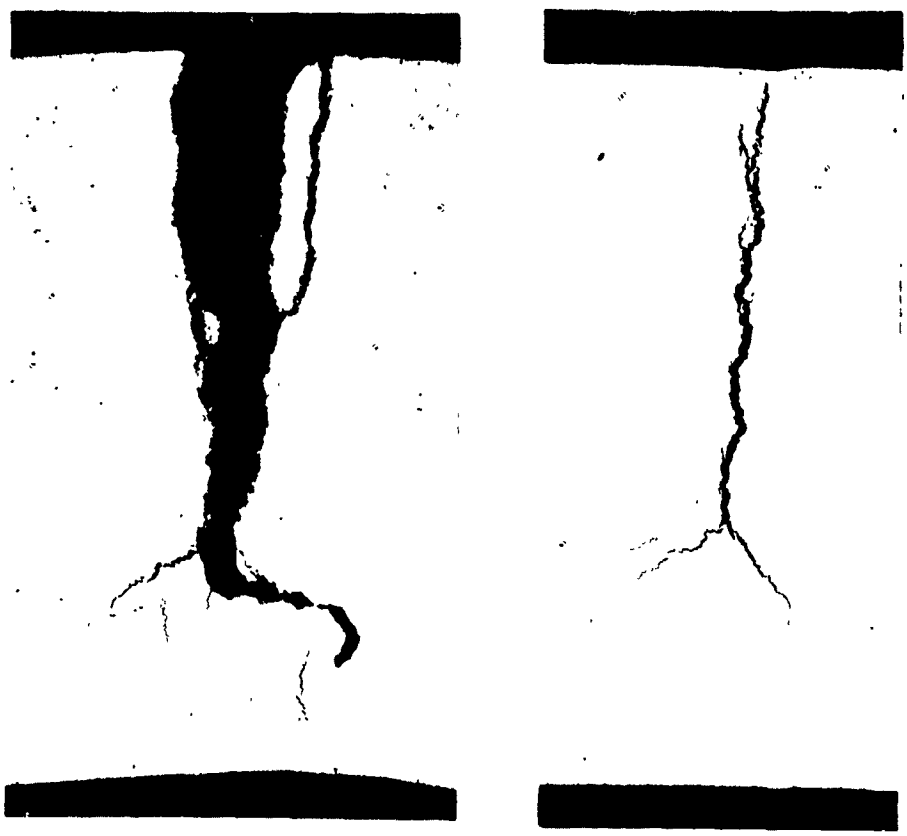

Longitudinal Section Through Cracked Area Showing Main Crack (left) and Branch Crack (5X)

Stress-Corrosion-Crack Pattern in 18%-Nickel Maraging Steel

Figure 13

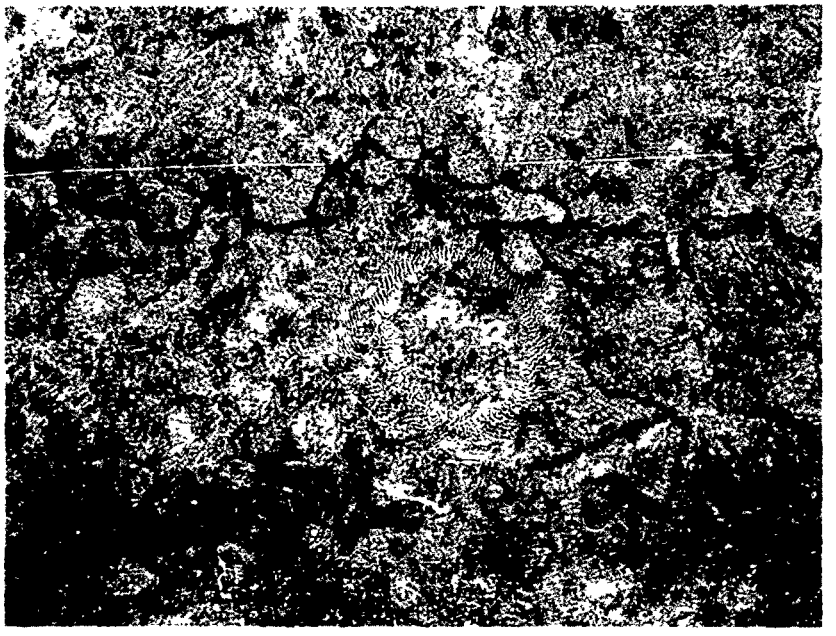

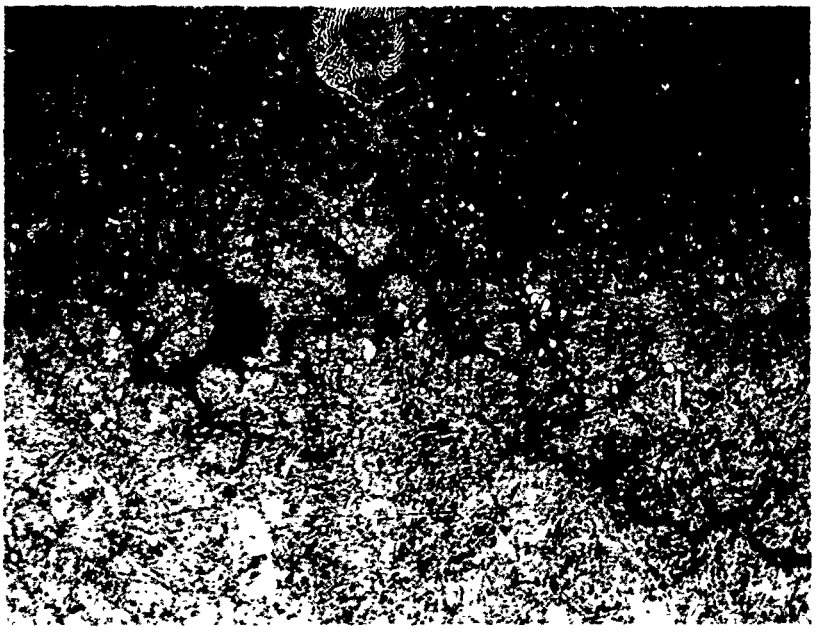

Typical Stress-Corrosion Cracks in Conventional High-Strength Steels

(Top) Low alloy steel Heat W-23217

(Bottom) Hot worked die steel Heat 07914

Etchant: HCl picral

Magnification: 500X

Figure 14

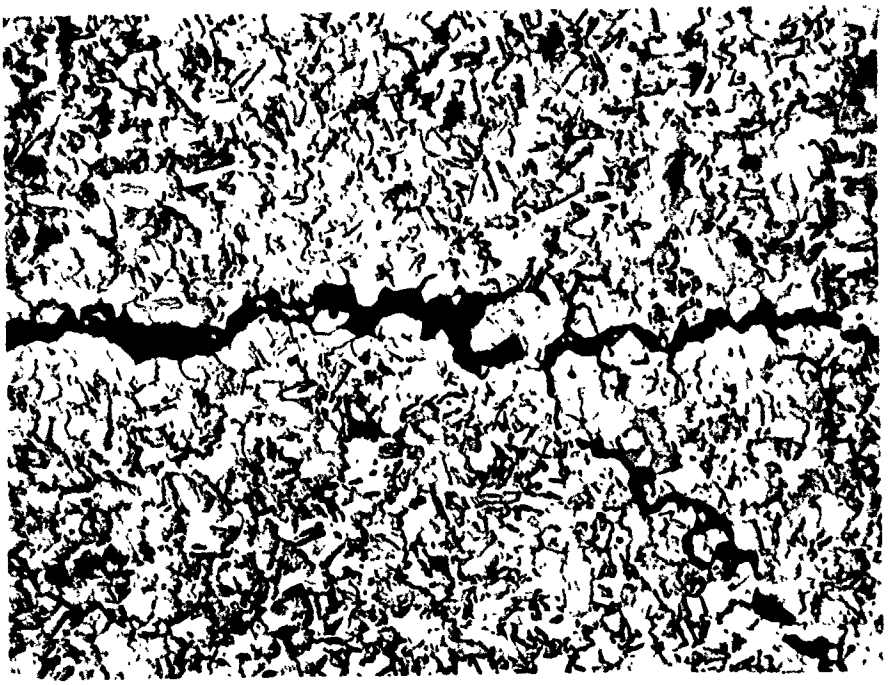

Vertical Section of Failed Annealed-and-Aged 18%-Nickel Maraging Steel Specimen Showing Intergranular Cracks. Marbles Etch (250X)

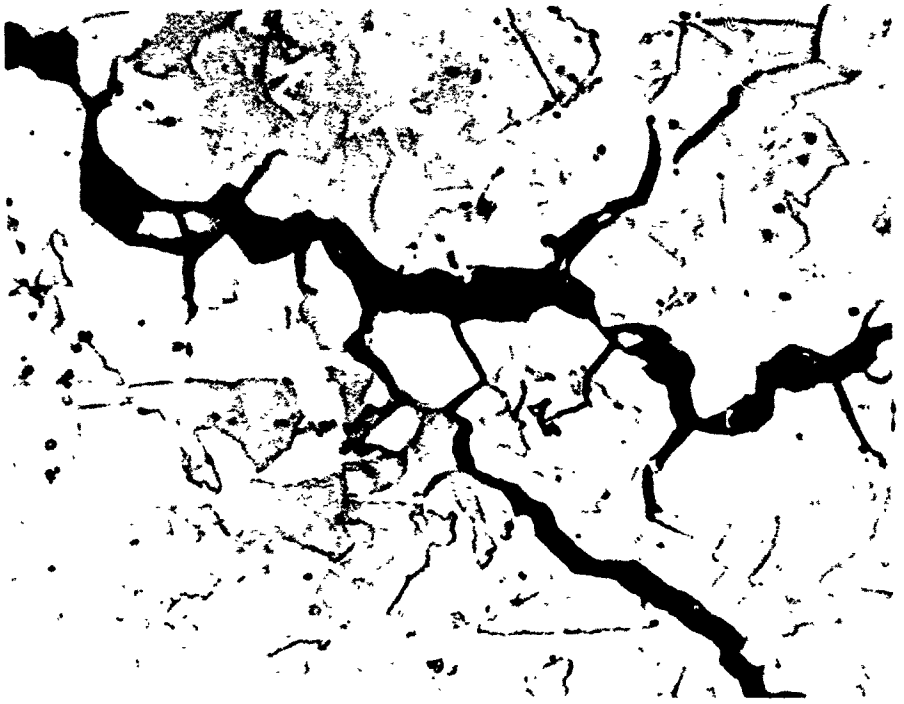

Same Sample as Above (2000X)

Photomicrographs of Stress-Corrosion Cracks in 18%-Nickel Maraging Steel

Figure 15

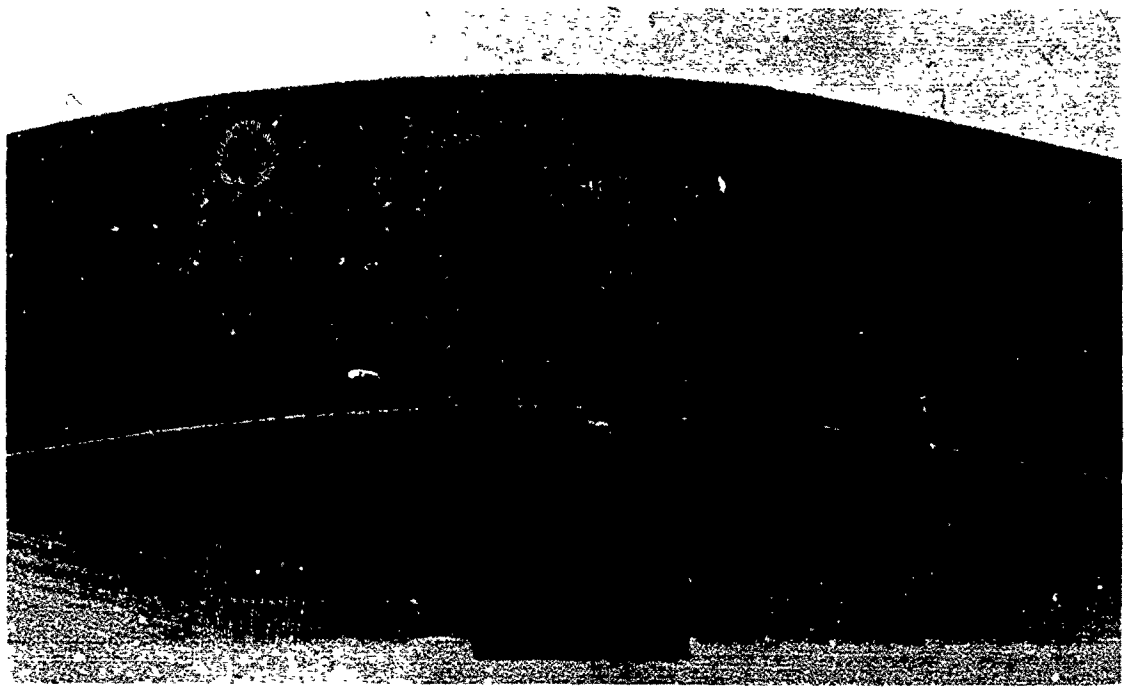

Surface of Cold-Worked-and-Aged 18%-Nickel Maraging Steel After 10-Days at 140°F in High Humidity Stress Corrosion Test. Surface has been Wire-Brushed. (Approx. 2X)

Cross-Section of Above Sample Showing Possible Cracking Along Slip Planes. (10X)

Stress-Corrosion-Crack Pattern in 18%-Nickel Maraging Steel

Figure 16

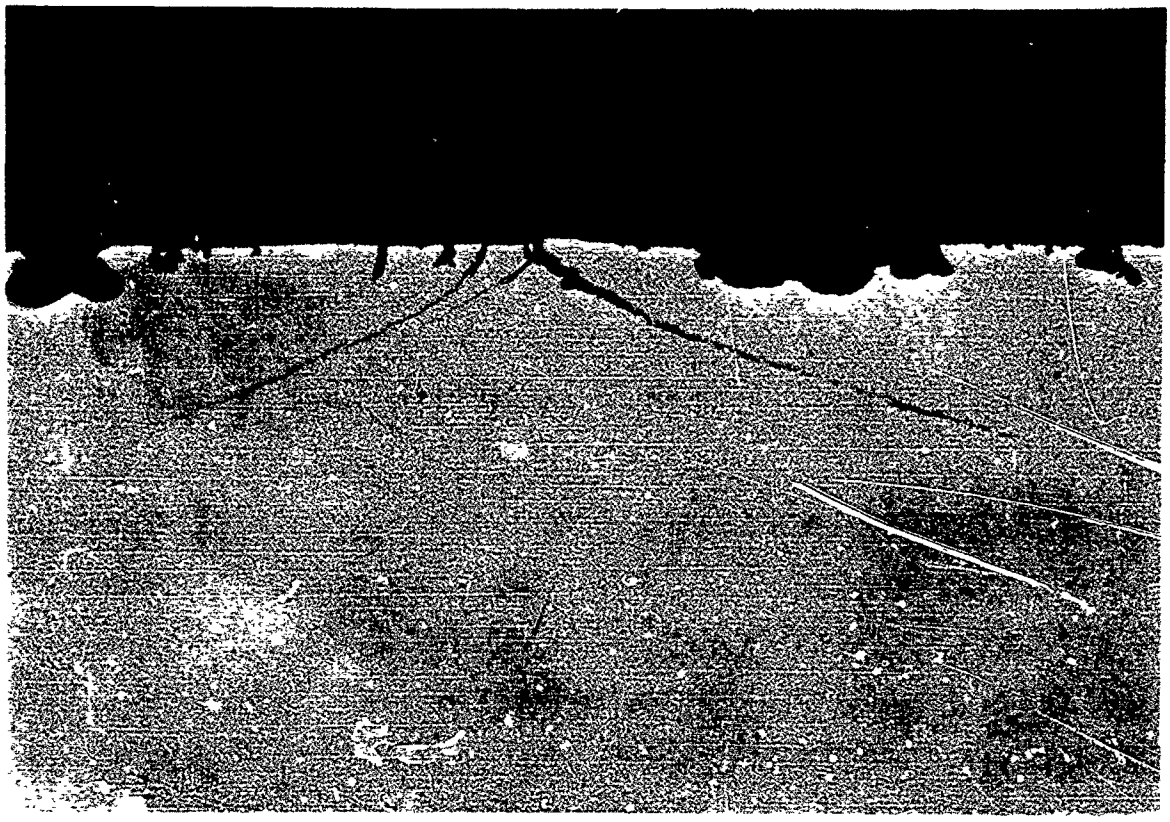

View of Surface in Lightly Cracked Area Showing Pitting Attack (100X)

General Structure in Interior of Highly Cracked Area.
Etchant - 10% Ammonium Persulphate-electrolytic. (500X)

Photomicrographs of Stress-Corrosion Cracking in 18%-Nickel Maraging Steel

Figure 17

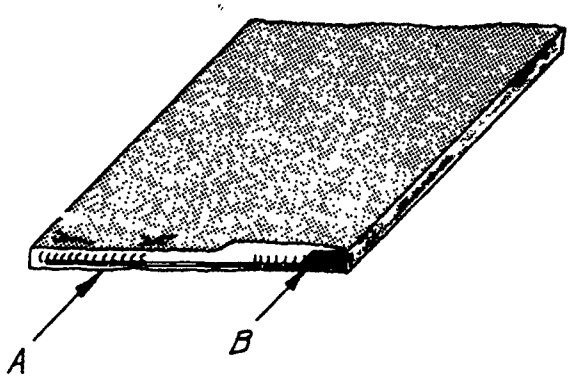

Uncoated H-11 Steel, Failed in 2.5 Hours in Aerated 3% Salt Water

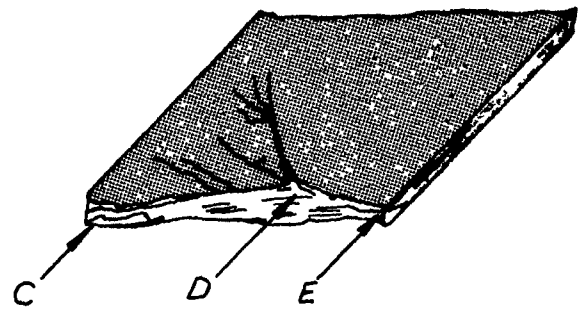

20%-Nickel Maraging Steel (Group H-1), Failed in 1 Hour in 0.25%-Sodium-Dichromate Solution

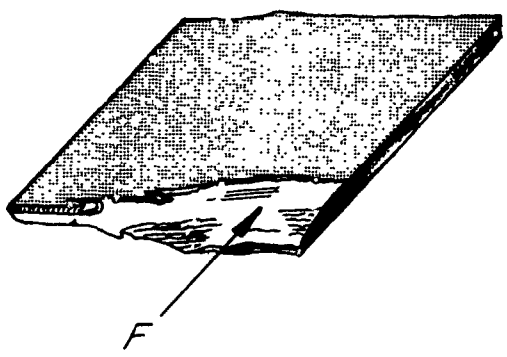

18%-Nickel Maraging Steel (Group I-3), Failed in 626 Hours in Aerated Distilled Water

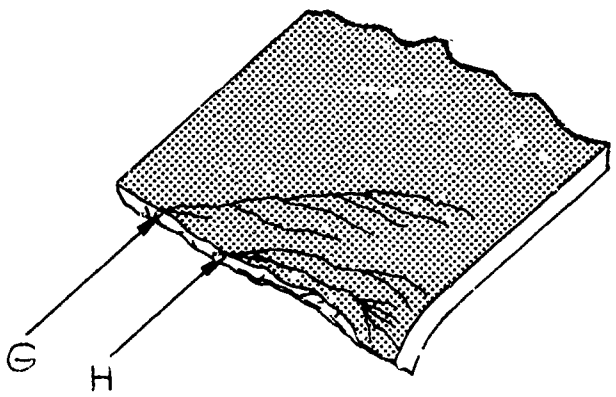

18%-Nickel Maraging Steel (Group I-1), Failed in 100 Hours in 0.25% Sodium Dichromate Solution

Location of Electron-Microscope Fractographs

Figure 18

Electron-Microscope Fractograph (1) of H-11 Steel (17,500X)

FIG - 19

Electron-Microscope Fractograph (2) of H-11 Steel (35,000X)

FIG - 20

Report No. 2914

Electron-Microscope Fractograph (1) of 18% Nickel Maraging Steel (17,500X)

FIG-21

Report No. 2419

Figure 21

Electron-Microscope Fractograph (2) of 18% Nickel Maraging Steel (20,000X)

Figure 22

Electron-Microscope Fractograph (3) of 18% Nickel Maraging Steel (20,000X)

Figure 23

45